Supporting Information

Coordination of hydrogen-bond and π-π stacking induced elasticity and efficient optical-waveguide of 4,7-bis(phenylethynyl)benzo[c][1,2,5]thiadiazole-based crystals

Geng Li[1], Yan Xia[1], Kunpeng Guo[1], Jie Li[1*], Yongli Yan[2*], Yoshimitsu Sagara[3], Yongzhen Yang[1*]

[1] *Ministry of Education Key Laboratory of Interface Science and Engineering in Advanced Materials, Taiyuan University of Technology, Taiyuan, 030024, China*

[2] *Laboratory of Photochemistry, Institute of Chemistry, Chinese Academy of Sciences, Beijing, 100190, China*

[3] *Department of Materials Science and Engineering, Tokyo Institute of Technology, Meguro-ku, Tokyo 152-8552, Japan*

E-mail: lijie01@tyut.edu.cn

ylyan@iccas.ac.cn

yangyongzhen@tyut.edu.cn

Table of contents

I. Experimental

General Methods

All of the chemicals and solvents were used as received from Alfa Chemical Co. Ltd. without further purification. All oxygen or moisture-sensitive reactions were performed under a nitrogen atmosphere.

The ^{1}H (600 MHz) and ^{13}C (150 MHz) NMR spectra were recorded on a Bruker NMR 600 spectrometer with tetramethylsilane (TMS) as the internal reference and deuterated chloroform ($CDCl_3$) or deuterated dimethyl sulfoxide (DMSO-d_6) as the solvent. ^{1}H NMR chemical shifts are reported in parts per million (ppm) relative to the solvent residual peak ($CDCl_3$, 7.26 ppm). Multiplicities are given as s (singlet), d (doublet), t (triplet), q (quartet), dd (doublet of doublets), dt (doublet of triplets), and m (multiplet), and the coupling constants *J* are given in Hz. ^{13}C NMR chemical shifts are reported relative to the solvent residual peak ($CDCl_3$, 77.36 ppm). MALDI-TOF mass spectrometry was performed using a Waters MALDI Micro MX mass spectrometer. Elemental analyses were performed on a Vario EL III elemental analyzer. UV-vis absorption spectra were obtained using a Hitachi U-3900 spectrometer. Photoluminescence spectra were taken on an Edinburgh Instrument FLS980 spectrometer equipped with a xenon lamp. The absolute fluorescence quantum yields of the samples were measured using an integrating sphere. The transient photoluminescence decay profiles were recorded using an Edinburgh Instrument FLS980 spectrometer equipped with an EPL-375 picosecond pulsed diode laser. Single crystal X-ray diffraction data were collected on a XtaLAB Synergy R, DW system, HyPix diffractometer at 301.95 K during data collection. The structures were solved by using Olex2 with the SHELXT structure solution program using Intrinsic Phasing and refined with the SHELXL refinement package using Least Squares minimization.

Synthesis and characterization

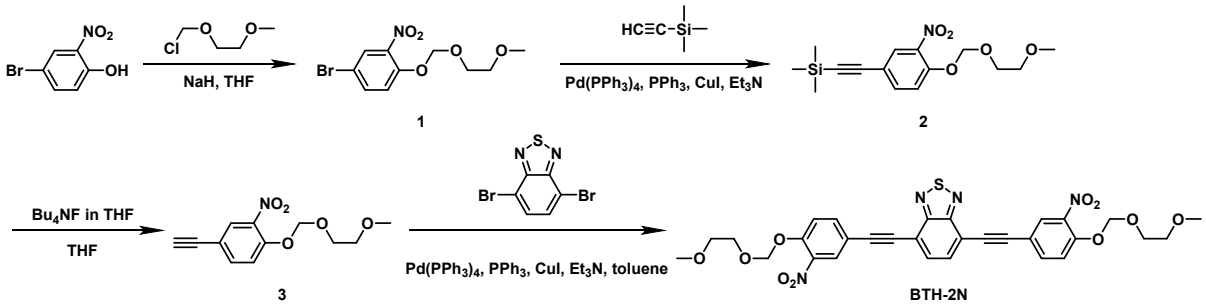

Scheme S1. Synthetic route to compound **PEBTH-2N**.

Synthesis of intermediate 4-bromo-1-(2-methoxyethoxymethoxy)-2-nitrobenzene (1)

To a solution of 4-bromo-2-nitrophenol (2.0 g, 9.17 mmol) and 2-methoxyethoxymethyl chloride (5.7 g, 45.76 mmol) in tetrahydrofuran (50 mL) was added sodium hydride (0.5 g, 0.021 mol) at 0 °C. The mixture was stirred at room temperature for 10 hours. Then the solvent was evaporated under reduced pressure and the residue was dissolved in dichloromethane. The organic phase was washed with saturated NaCl solution, dried over $MgSO_4$, and filtered. After concentrated under reduced pressure, the crude product was purified by column chromatography (petroleum ether/ethyl acetate 20/1 v/v) to yield **1** as a yellowish oil (2.53 g, 8.265 mmol, 90% yield). ^{1}H NMR (600 MHz, $CDCl_3$) δ 7.93 (d, J = 2.5 Hz, 1H), 7.61 (dd, J = 9.0, 2.5 Hz, 1H), 7.29 (d, J = 9.0 Hz, 1H), 5.38 (s, 2H), 3.88 – 3.86 (m, 2H), 3.57 – 3.54 (m, 2H), 3.36 (s, 3H). ^{13}C NMR (101 MHz, $CDCl_3$) δ 149.44, 140.96, 136.59, 127.78, 119.02, 113.14, 94.35, 71.28, 68.50, 58.82.

Synthesis of intermediate ((4-(2-methoxyethoxymethoxy)-3-nitrophenyl)ethynyl)trimethylsilane (2)

To triethylamine (20 mL) solution was added compound **1** (1.0 g, 3.27 mmol), trimethylsilylacetylene (0.638 g, 6.49 mmol), triphenylphosphine (0.06 g, 0.23 mmol), cuprous iodide (0.02 g, 0.11 mmol), and tetrakis-(triphenylphosphine)-palladium (0.06 g, 0.05 mmol), successively. The reaction mixture was stirred at 65 °C for 5 hours. After cooling to room temperature, the solvent was evaporated under reduced pressure and the residue was dissolved in dichloromethane. The solution was washed with saturated NaCl solution, dried over $MgSO_4$ and filtered. After concentrated under reduced pressure, the crude product was purified by

column chromatography (petroleum ether/ethyl acetate 20/1 v/v) to yield **2** as a yellowish oil (0.96 g, 2.97 mmol, 90% yield). ^{1}H NMR (600 MHz, $CDCl_3$) δ 7.65 (d, J = 1.9 Hz, 1H), 7.32 (dd, J = 8.7, 2.0 Hz, 1H), 7.05 (d, J = 8.7 Hz, 1H), 5.15 (s, 2H), 3.64 – 3.60 (m, 2H), 3.32 – 3.27 (m, 2H), 3.11 (s, 3H), 0.00 (s, 9H). ^{13}C NMR (101 MHz, CDCl3) δ 150.30, 140.40, 137.20, 128.83, 117.22, 117.12, 102.28, 95.82, 94.34, 71.53, 68.75, 59.13, 0.00.

Synthesis of intermediate 4-ethynyl-1-(2-methoxyethoxymethoxy)-2-nitrobenzene (3)

To tetrahydrofuran (10 mL) solution was added compound **2** (1.0 g, 3.09 mmol) and tetrabutylammonium fluoride (1 mol/L, 4.195 mmol) solution, the reaction mixture was stirred at room temperature in the dark for about 3 hours. Then the solvent was evaporated under reduced pressure and the residue was dissolved in dichloromethane. The solution was washed with saturated NaCl solution, dried over $MgSO_4$, and filtered. After concentrated under reduced pressure, the crude product was purified by column chromatography (petroleum ether/ethyl acetate 20/1 v/v) to yield **3** as a yellowish oil (0.66 g, 2.63 mmol, 85% yield). ^{1}H NMR (600 MHz, $CDCl_3$) δ 7.92 (d, J = 1.8 Hz, 1H), 7.60 (dd, J = 8.7, 1.9 Hz, 1H), 7.33 (d, J = 8.7 Hz, 1H), 5.40 (s, 2H), 3.88 – 3.86 (m, 2H), 3.56 – 3.54 (m, 2H), 3.36 (s, 3H), 3.10 (s, 1H). ^{13}C NMR (151 MHz, $CDCl_3$) δ 150.39, 140.19, 137.23, 128.77, 117.14, 115.71, 94.13, 80.94, 78.46, 71.29, 68.57, 58.88.

Synthesis of and 4,7-bis((4-(2-methoxyethoxymethoxy)-3-nitrophenyl)ethynyl)benzo[c][1,2,5]thiadiazole (PEBTH-2N)

To triethylamine (10 mL) and toluene (23 mL) solution was added 4,7-dibromobenzo[c][1,2,5]thiadiazole (0.53 g, 1.81 mmol), triphenylphosphine (0.008 g, 0.1 mmol), cuprous iodide (0.008 g, 0.04 mmol), tetrakis-(triphenylphosphine)-palladium (0.025 g, 0.021 mmol) , and compound **3** (1.0 g, 3.98 mmol), successively. The reaction mixture was stirred at 70 °C for 5 h. After cooling to room temperature, the solvent was evaporated under reduced pressure and the residue was dissolved in dichloromethane. Then the solution was washed with saturated NaCl solution, dried over $MgSO_4$ and filtered.

After concentrated under reduced pressure, the crude product was purified by column chromatography (dichloromethane /ethyl acetate 2/1 v/v) to yield **PEBTH-2N** as a yellow powder (1.226 g, 1.93 mmol, 58% yield). ^{1}H NMR (600 MHz, $CDCl_3$) δ 8.12 (d, *J* = 2.2 Hz, 2H), 7.81 (s, 2H), 7.79 (dd, *J* = 8.7, 2.1 Hz, 2H), 7.44 – 7.39 (m, 2H), 5.45 (s, 4H), 3.93 – 3.89 (m, 4H), 3.60 – 3.55 (m,4H), 3.38 (s, 6H).^{13}C NMR (151 MHz, $CDCl_3$) δ (ppm) 154.20, 150.70, 140.40, 137.11, 132.59, 128.75, 117.24, 116.91, 116.14, 94.81, 94.19, 86.08, 71.35, 68.68, 59.04. MS (MALDI-TOF/TOF): m/z calcd. for $C_{30}H_{26}N_4O_{10}S$ 634.62, found 657.118 $[M+Na]^+$.

Theoretical calculation

The transition dipole moment (μ) was calculated using the time-dependent density functional theory (TD-DFT) calculations at the B3LYP/6-31G(d) level using the Gaussian 09W program package. The molecular skeleton selected from the 1D needle-like crystal.

Crystal growth

1D needle-like crystals: **PEBTH-2N** (2 mg) was dissolved in the mixed solvents (1.5 mL, ethyl acetate/acetonitrile 2/1 v/v), which was then placed in a vial with unscrewed cap. Yellow crystals were obtained within one week at at room temperature.

Curved crystals: **PEBTH-2N** (2 mg) was dissolved in dichloromethane (1.5 mL), which was then placed in a vial with unscrewed cap. The key process to cultivate curved crystals is preplacing a few mini crystal seeds in the bottom of the vial, then keeping the mixture in slow growth. Orange crystals were obtained within one week at room temperature.

II. Structures and photophysical properties of the compound

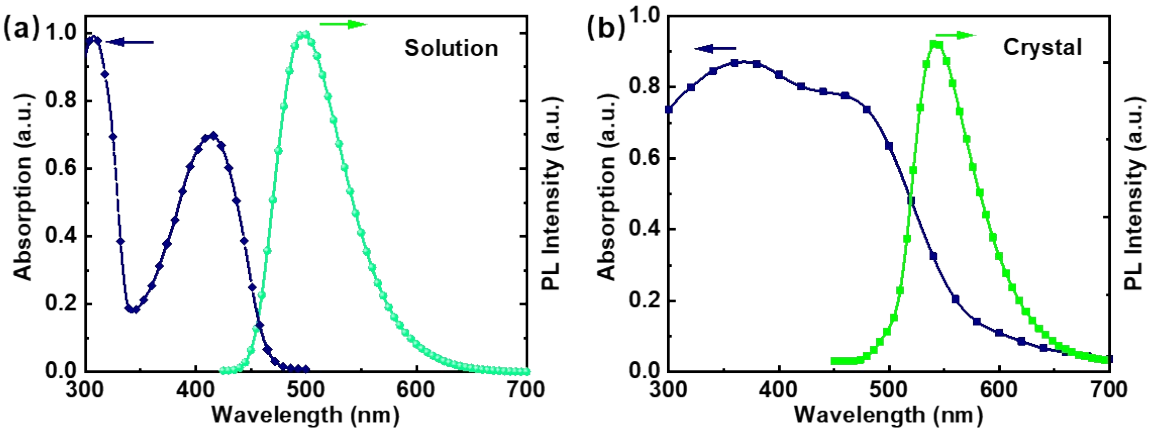

Fig. S1 UV−vis absorption and PL spectra of **PEBTH-2N** in (a) dichloromethane (10^{-5} M, ε = 87000) and (b) crystal cultivated from ethyl acetate and acetonitrile.

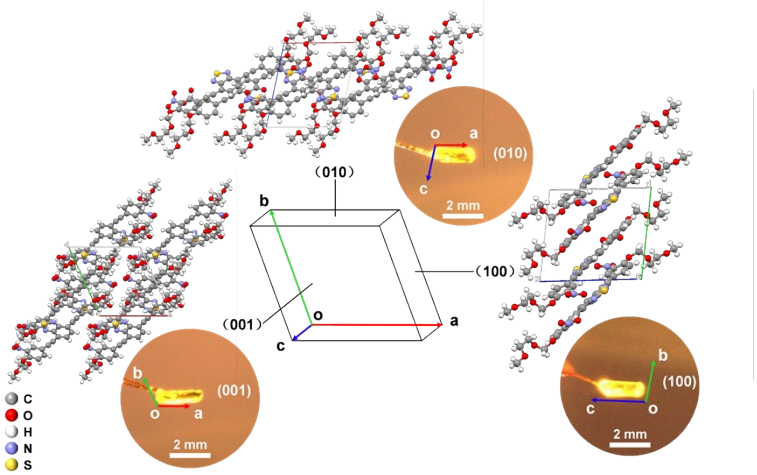

Fig. S2 Images of a **PEBTH-2N** single crystal and packing diagrams viewed down the major faces of the crystals.

Table S1. Fluorescence properties and structural data of isostructural polymorphs of **PEBTH-2N** obtained from various solvents

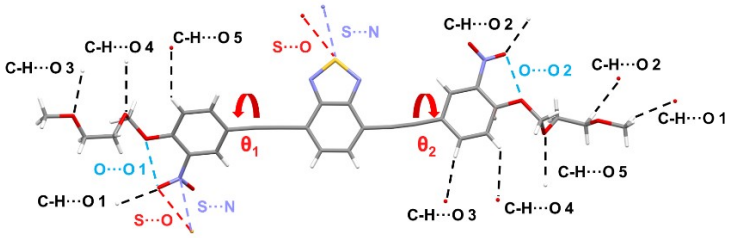

Fluorescence	519 nm		543 nm	545 nm		554 nm
Solvent / Parameter	ACN	DCM+ACN	EAC+ACN	EAC+EtOH	DCM+EtOH	DCM+HEX
θ_1 (°)	24.27	24.24	24.09	24.09	24.04	23.78
θ_2 (°)	2.27	2.27	2.26	2.14	2.35	2.42
O-O 1 (Å)	2.613	2.614	2.616	2.613	2.606	2.609
O-O 2 (Å)	2.667	2.668	2.67	2.663	2.662	2.669
S-N (Å)	3.371	3.379	3.381	3.379	3.383	3.380
S-O (Å)	3.312	3.314	3.315	3.316	3.314	3.317
π-π (Å)	3.131	3.132	3.132	3.129	3.14	3.122
CH-O 1 (Å)	2.442	2.442	2.454	2.444	2.435	2.438
CH-O 2 (Å)	2.716	2.712	2.714	2.711	2.72	2.715
CH-O 3 (Å)	2.584	2.59	2.593	2.594	2.59	2.595
CH-O 4 (Å)	2.694	2.704	2.704	2.709	2.713	2.706
CH-O 5 (Å)	2.659	2.661	2.661	2.66	2.663	2.666

The abbreviation for the solevents:

ACN: acetonitrile; DCM: dichloromethane; EAC: ethyl acetate; EtOH: ethanol; HEX: hexane

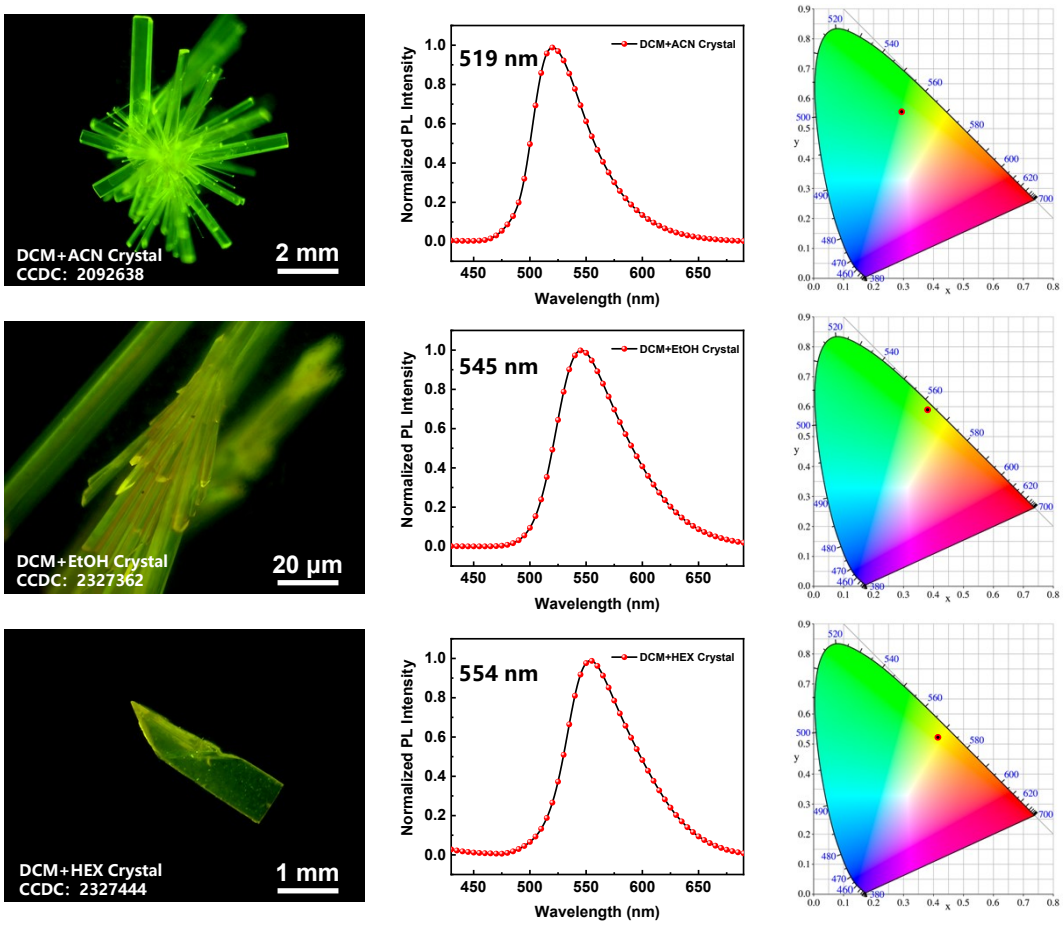

Fig. S3 Fluorescence microscopy images and corresponding PL spectra and CIE coordinates of **PEBTH-2N** crystals with typical morphologies obtained from different solvents.

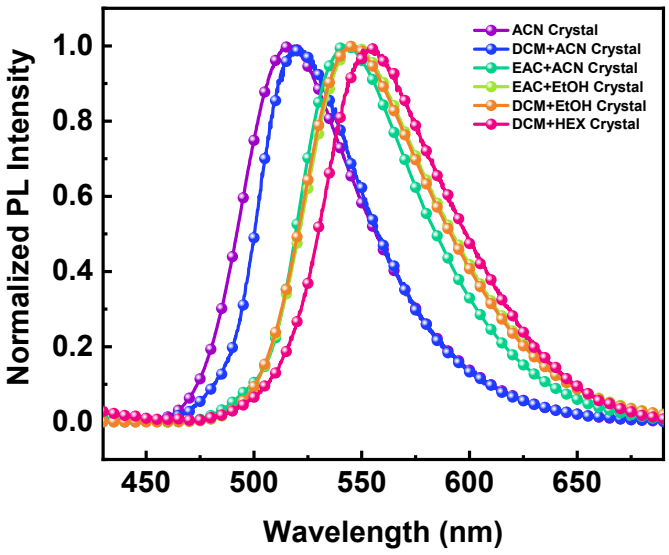

Fig. S4 PL spectra of **PEBTH-2N** crystals obtained from various solvents.

III. Calculated transition dipole moment of PEBTH-2N

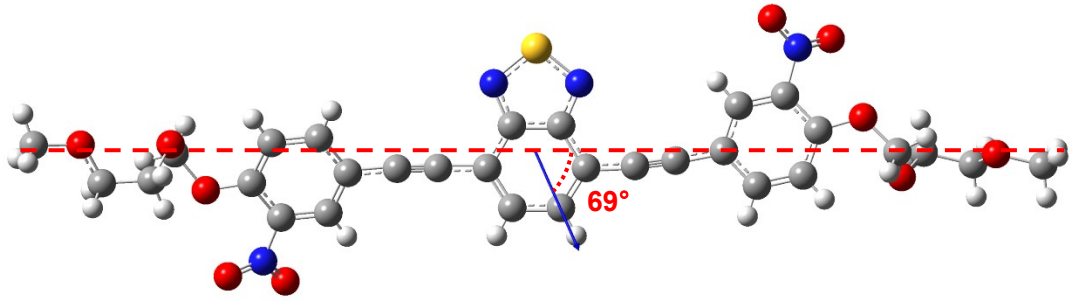

Fig. S5 Calculated transition dipole moment of the molecule in the1D needle-like crystal

IV. The PL spectra of a bendable crystal after each bending recovery

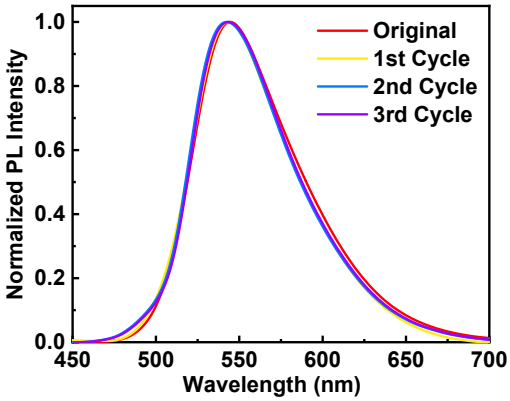

Fig. S6 The PL spectra of a bendable crystal after each bending recovery

V. Photophysical properties of the straight and curved crysals

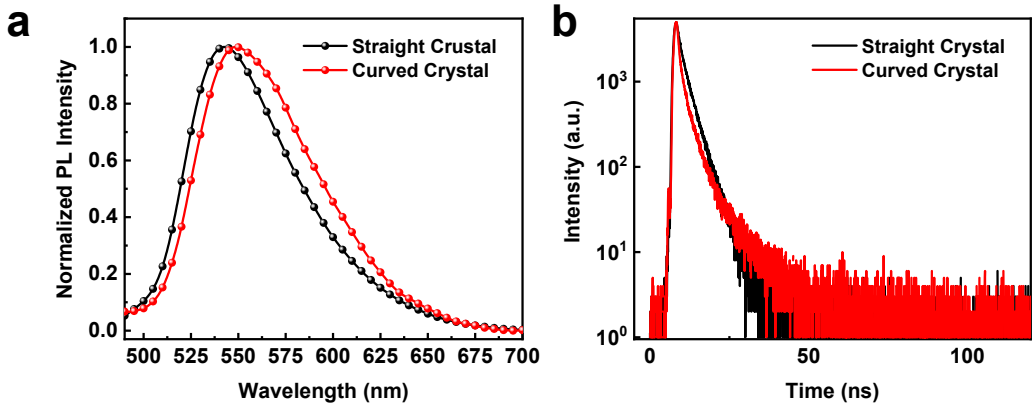

Fig. S7 (a) PL spectra and **(b)** time-resolved fluorescence decay profiles of the straight and cured crystals of **PEBTH-2**

Table S2. Photophysical properties of the straight needle-like crystal and the curved crystal

Crystal	λ_{PL} (nm)	τ (ns)	PLQY (%)	k_r (s^{-1})	k_{nr} (s^{-1})
Straight	543	2.61	15.2	5.8×10^7	3.2×10^8
Curved	550	2.73	5.0	1.8×10^7	3.5×10^8

VI. Crystal data of the crystals

Fluorescence	519 nm	543 nm	543 nm	545 nm	545 nm	554 nm
Solvent	ACN	DCM+ACN	EAC+ACN	EAC+EtOH	DCM+EtOH	DCM+HEX
CCDC No.	2327442	2092638	2172217	2327445	2327362	2327444
Empirical formula	$C_{30}H_{26}N_4O_{10}S$	$C_{30}H_{26}N_4O_{10}S$	$C_{30}H_{26}N_4O_{10}S$	$C_{30}H_{26}N_4O_{10}S$	$C_{30}H_{26}N_4O_{10}S$	$C_{30}H_{26}N_4O_{10}S$
Formula weight	634.61	634.61	634.61	634.61	634.61	634.61
Temperature/K	293(2)	293(2)	293(2)	293(2)	293(2)	293(2)
Crystal system	triclinic	triclinic	triclinic	triclinic	triclinic	triclinic
Space group	P-1	P-1	P-1	P-1	P-1	P-1
a/Å	11.3990(5)	11.3999(3)	11.4078(2)	11.4091(3)	11.3944(7)	11.4076(5)
b/Å	11.9349(5)	11.9421(4)	11.95220(19)	11.9500(3)	11.9308(8)	11.9590(5)
c/Å	12.3406(6)	12.3472(3)	12.3521(2)	12.3526(3)	12.3382(7)	12.3522(6)
α/°	92.5870(10)	92.589(2)	92.5996(14)	92.6180(10)	92.546(5)	92.643(2)
β/°	100.4110(10)	100.370(2)	100.3827(15)	100.3390(10)	100.445(5)	100.271(2)
γ/°	113.535(2)	113.532(3)	113.5545(16)	113.5900(10)	113.502(6)	113.6630(10)
Volume/Å^3	1501.03(12)	1503.15(8)	1505.66(5)	1505.39(7)	1499.96(17)	1505.71(12)
Z	2	2	2	2	2	2
ρ_{calc}g/cm^3	1.404	1.402	1.400	1.574	1.405	1.400
μ/mm^{-1}	0.173	0.173	1.516	0.753	0.173	0.172
F(000)	660.0	660.0	660.0	722.0	660.0	660.0
Crystal size/mm^3	0.18 × 0.12 × 0.05	0.08 × 0.04 × 0.02	0.11 × 0.08 × 0.05	0.15 × 0.08 × 0.05	0.04 × 0.03 × 0.02	0.15 × 0.1 × 0.04
Radiation	MoKα (λ =	Mo Kα (λ =	CuKα (λ =	MoKα (λ =	Mo Kα (λ =	MoKα (λ =

	0.71073)	0.71073)	1.54184)	0.71073)	0.71073)	0.71073)
2Θ range for data collection/°	5.372 to 56.38	3.382 to 61.992	7.338 to 152.638	3.752 to 56.602	3.386 to 61.936°	5.144 to 56.458
Index ranges	-15 ≤ h ≤ 15, -14 ≤ k ≤ 15, -16 ≤ l ≤ 16	-14 ≤ h ≤ 15, -16 ≤ k ≤ 15, -17 ≤ l ≤ 15	-14 ≤ h ≤ 14, -15 ≤ k ≤ 14, -14 ≤ l ≤ 15	-15 ≤ h ≤ 15, -15 ≤ k ≤ 15, -16 ≤ l ≤ 16	-15 ≤ h ≤ 13, -16 ≤ k ≤ 15, -17 ≤ l ≤ 15	-15 ≤ h ≤ 15, -15 ≤ k ≤ 12, -16 ≤ l ≤ 16
Reflections collected	15606	20183	18803	37280	17561	15648
Independent reflections	7203 [Rint = 0.0312, Rsigma = 0.0412]	7501 [R_{int} = 0.0199, R_{sigma} = 0.0254]	6030 [R_{int} = 0.0341, R_{sigma} = 0.0344]	7430 [Rint = 0.0401, Rsigma = 0.0291]	7215 [Rint = 0.0629, Rsigma = 0.0912]	7252 [Rint = 0.0329, Rsigma = 0.0449]
Data/restraints/parameters	7203/0/408	7501/0/408	6030/0/408	7430/0/408	7215/0/408	7252/0/409
Goodness-of-fit on F^2	1.072	1.092	0.956	1.090	0.820	1.023
Final R indexes [I>=2σ(I)]	R_1 = 0.0628, wR_2 = 0.1862	R_1 = 0.0504, wR_2 = 0.1517	R_1 = 0.0573, wR_2 = 0.1649	R_1 = 0.0689, wR_2 = 0.1952	R_1 = 0.0676, wR_2 = 0.2035	R_1 = 0.0744, wR_2 = 0.2258
Final R indexes [all data]	R_1 = 0.0838, wR_2 = 0.2137	R_1 = 0.0706, wR_2 = 0.1641	R_1 = 0.0627, wR_2 = 0.1723	R_1 = 0.0939, wR_2 = 0.2203	R_1 = 0.1492, wR_2 = 0.2887	R_1 = 0.0999, wR_2 = 0.2577
Largest diff. peak/hole/eA^{-3}	0.54/-0.35	0.54/-0.34	0.45/-0.48	0.60/-0.62	0.41/-0.26	0.71/-0.35

VII. ^{1}H and ^{13}C NMR spectra

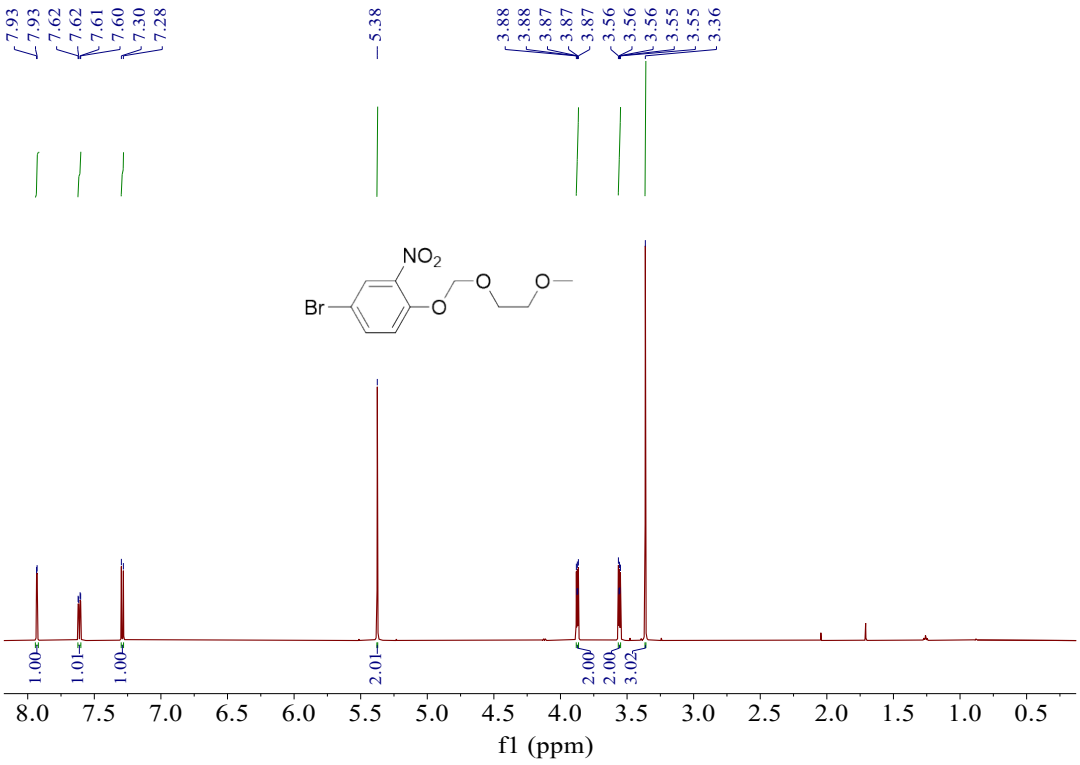

Fig. S7 ^{1}H NMR spectrum (600 MHz, $CDCl_3$) of **1**.

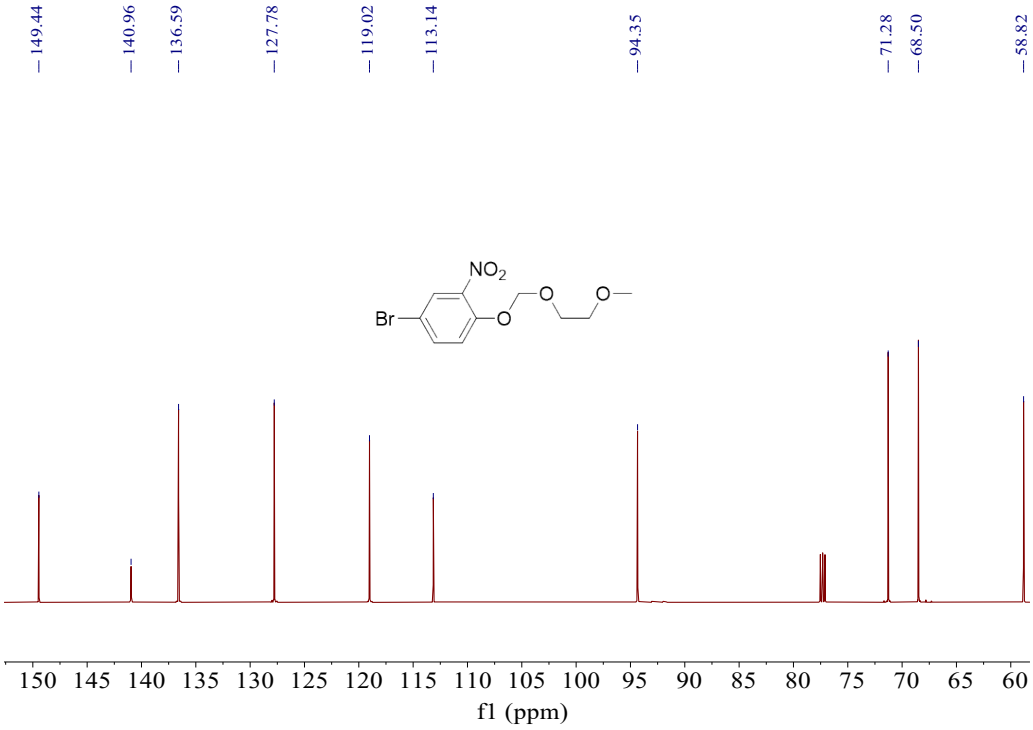

Fig. S8 ^{13}C NMR spectrum (101 MHz, $CDCl_3$) of **1**.

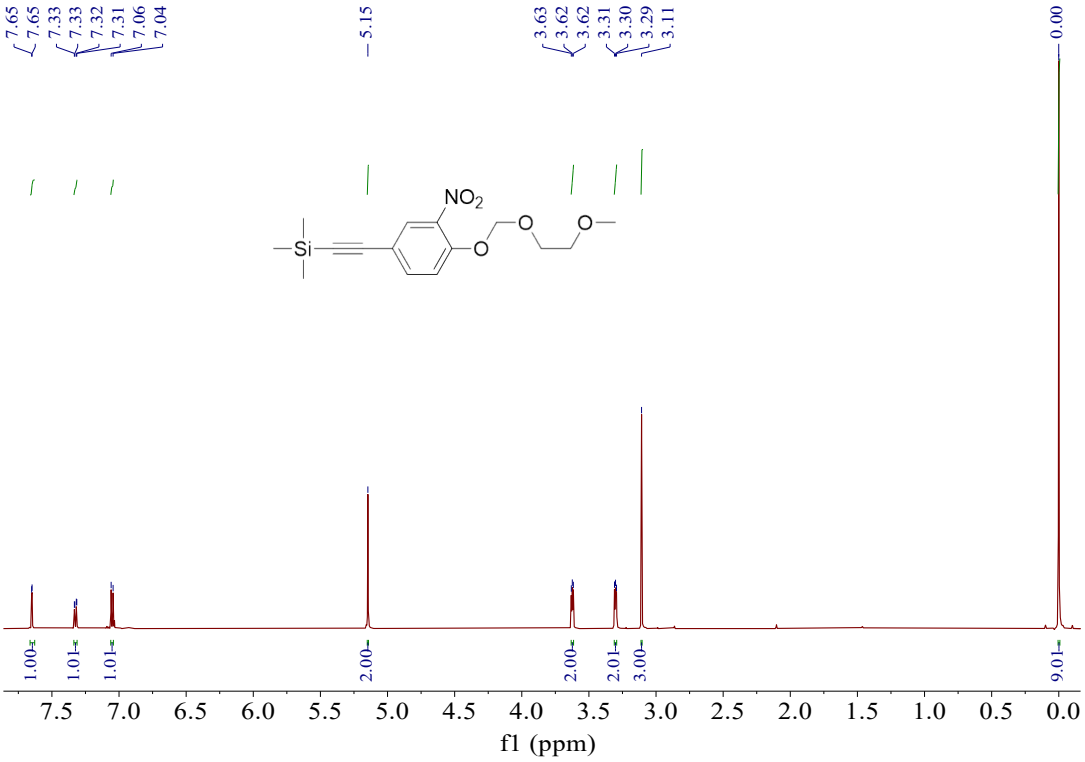

Fig. S9 ^{1}H NMR spectrum (600 MHz, $CDCl_3$) of **2**.

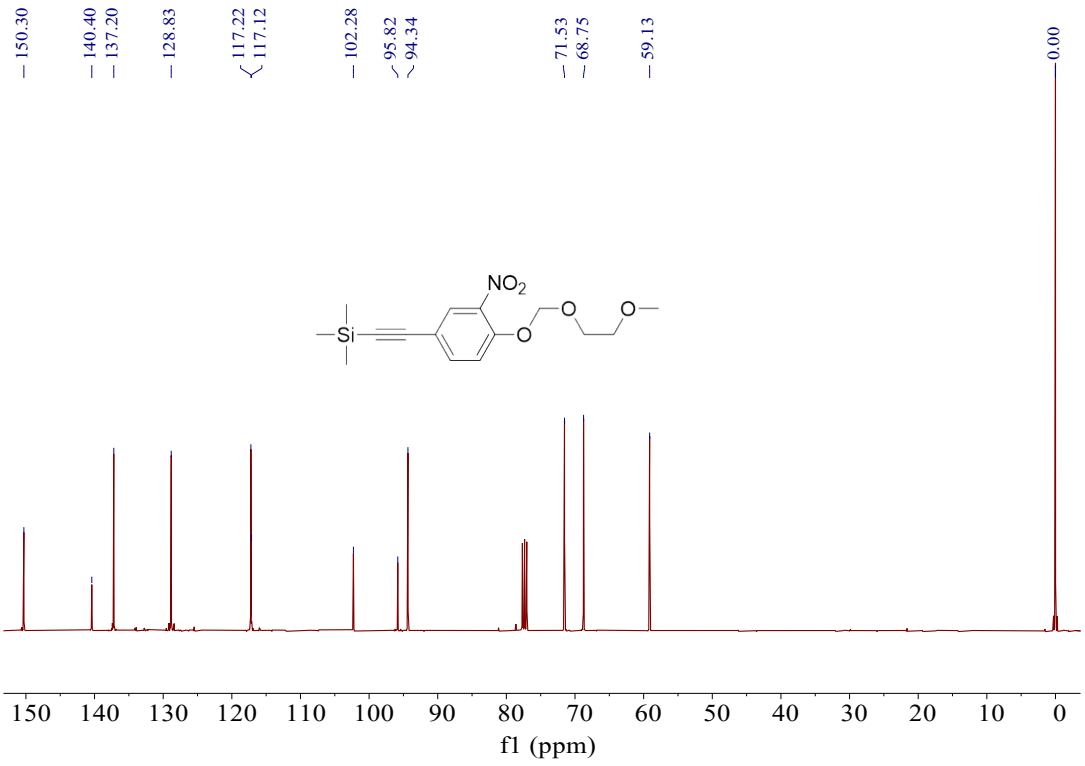

Fig. S10 ^{13}C NMR spectrum (101 MHz, $CDCl_3$) of **2**.

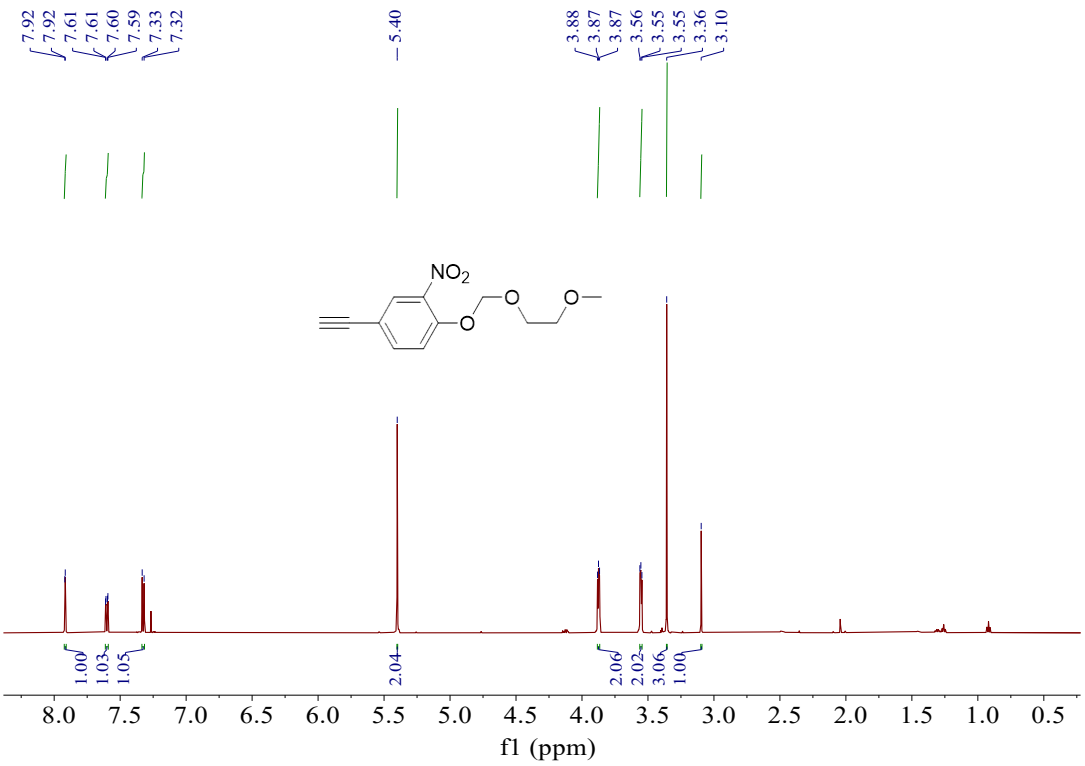

Fig. S11 ^{1}H NMR spectrum (600 MHz, $CDCl_3$) of **3**.

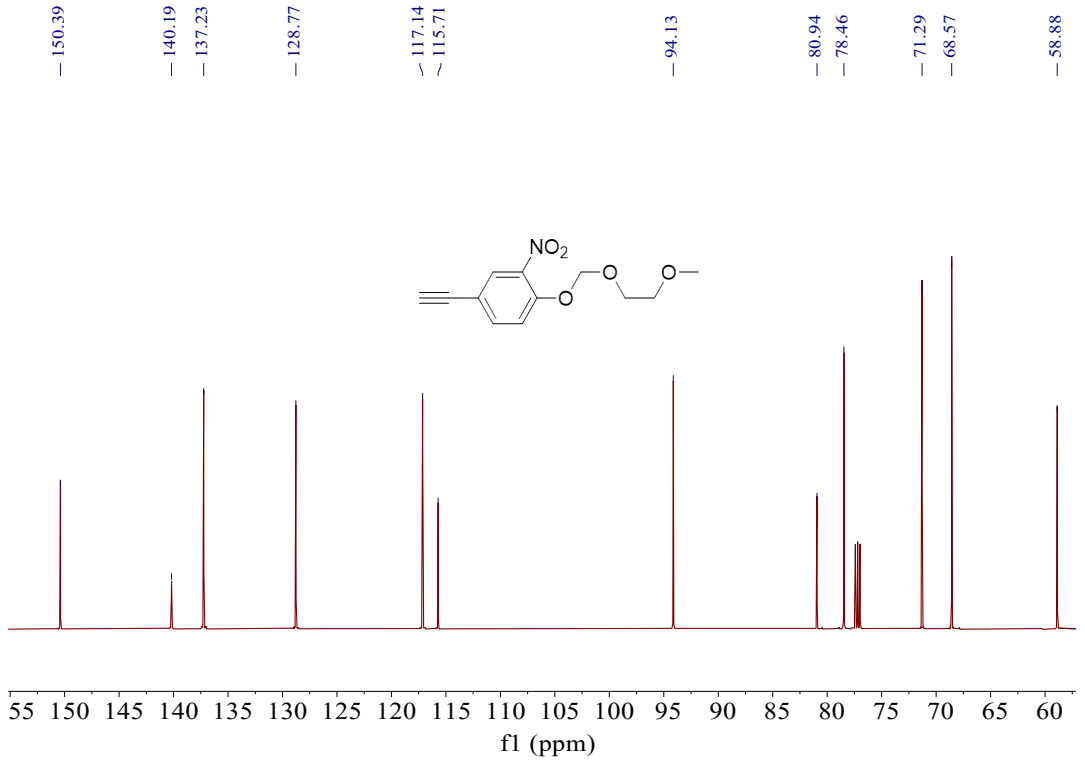

Fig. S12 ^{13}C NMR spectrum (151 MHz, $CDCl_3$) of **3**.

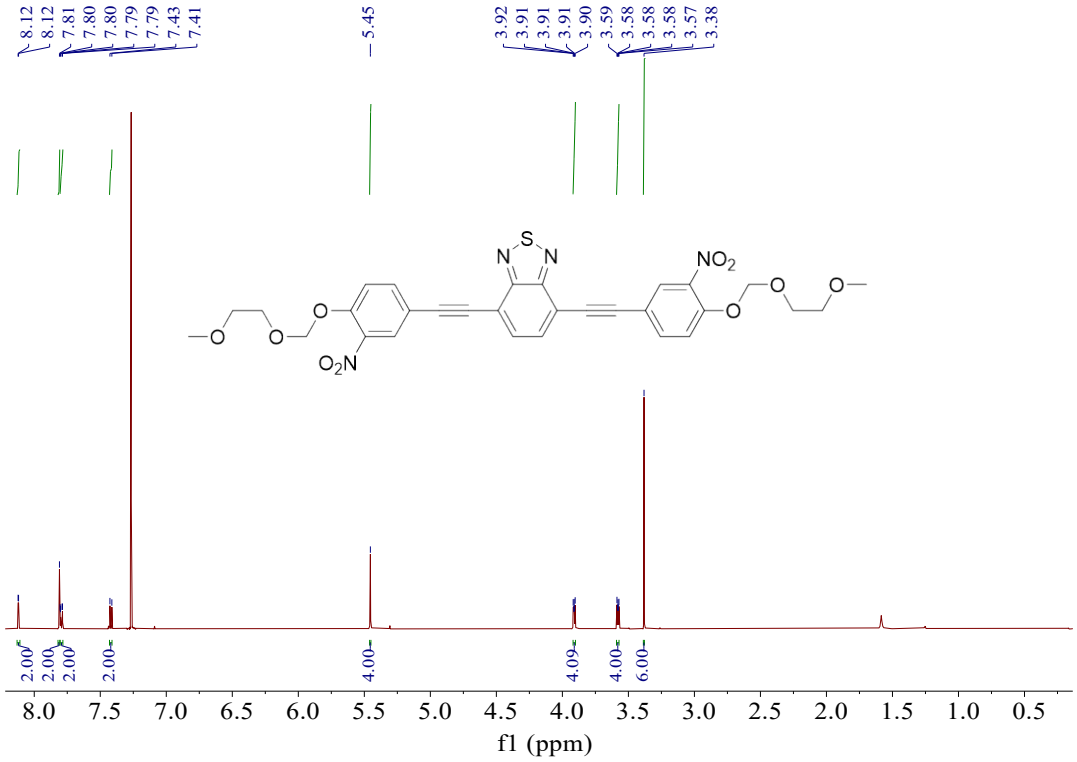

Fig. S13 ^{1}H NMR spectrum (600 MHz, $CDCl_3$) of **PEBTH-2N**.

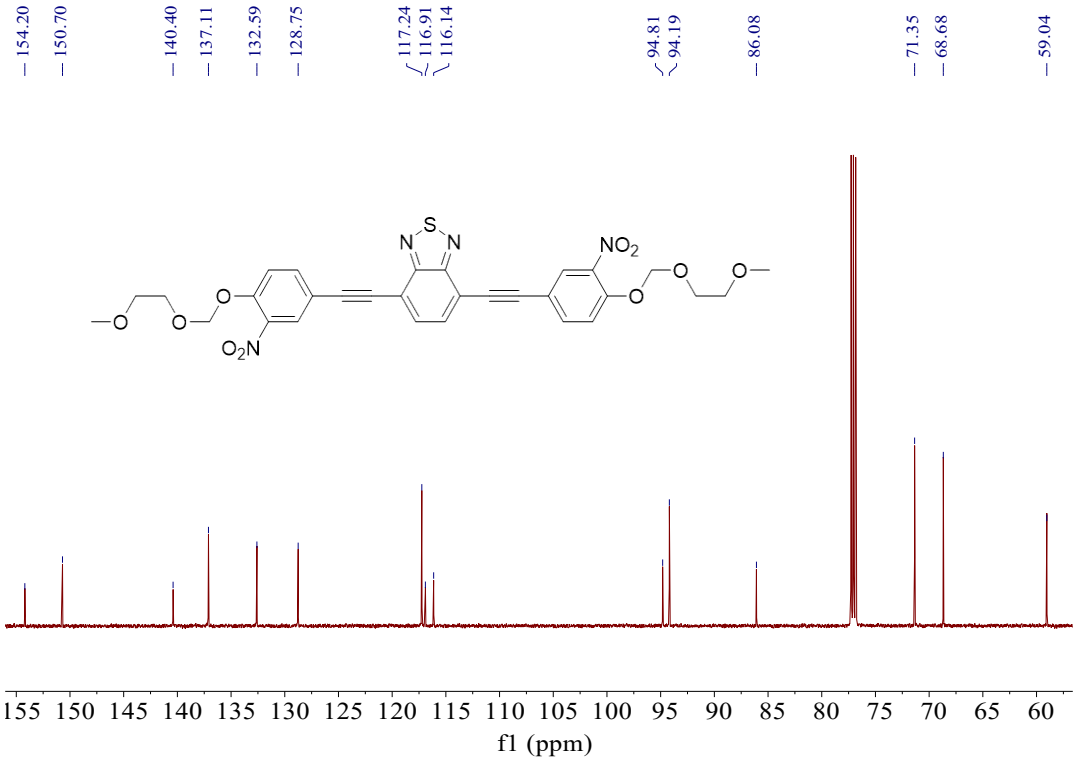

Fig. S14 ^{13}C NMR spectrum (151 MHz, $CDCl_3$) of **PEBTH-2N**.